Materials Today Bio 16 (2022) 100340

Contents lists available at ScienceDirect

Materials Today Bio

journal homepage: www.journals.elsevier.com/materials-today-bio

Differential effect of tantalum nanoparticles versus tantalum micron particles on immune regulation

Yan Sun [a,c], Tuozhou Liu [a,c], Hongkun Hu [a,c], Zixuan Xiong [a,c], Kai Zhang [a,c], Xi He [a,c], Wenbin Liu [a,c,***], Pengfei Lei [a,b,c,**], Yihe Hu [a,b,c,*]

[a] Department of Orthopedic Surgery, Xiangya Hospital, Central South University, Changsha, National Clinical Research Center of Geriatric Disorders, Xiangya Hospital, Central South University, Changsha, China
[b] Department of Orthopedics, The First Affiliated Hospital, Medical College of Zhejiang University, Hangzhou, PR China
[c] Hunan Engineering Research Center of Biomedical Metal and Ceramic Implants, Changsha, China

ARTICLE INFO

Keywords:
Tantalum nanoparticles
Tantalum micron particles
Macrophages
Inflammatory microenvironment

ABSTRACT

The inflammatory microenvironment created by macrophages has been proven critical for bone regeneration. Both tantalum nanoparticles and micron particles have been applied to bone tissue engineering and have achieved good efficacy, but their effects on immune microenvironment remain unclear. Herein, we explored the different effects between nano- and micro-tantalum particles on the innate immunity of macrophages *in vitro* and *in vivo*. RAW 264.7 cells were co-cultured with nano- and micro-tantalum particles under inflammatory conditions to evaluate the effects on the morphology and behavior of macrophages. Air pouch model was used to evaluate the material-induced macrophage polarization *in vivo*. Compared to the tantalum micron particles (TaMPs), the morphology of macrophages was more similar to the M2 phenotype in co-culture with tantalum nanoparticles (TaNPs). At the same time, the TaNPs could also decrease the gene expression of interleukin-1β (IL-1β), tumor necrosis factor-α(TNF-α), inducible nitric oxide synthase (iNOS), and increase the expression of transforming growth factor-β1 (TGF-β1) and interleukin-10 (IL-10). Furthermore, the air pouch model showed more M2 macrophage infiltration under the intervention of TaNPs. Our findings demonstrated that TaNPs could significantly increase the polarization of M2 macrophages and decrease the macrophage polarization to the M1 phenotype under the inflammatory microenvironment, showing better immunomodulatory properties.

1. Introduction

With the development of social economy and the aging of world population, there has also been a sharp increase in the incidence of many diseases such as fractures, spinal degeneration, arthritis and bone tumors. The clinical demand for bone implants is also increasing, and the manufacture and development of orthopedic implants has always been a hot direction and one of the key contents in the field of biomaterials research [1–3].

When biomaterials are implanted into the human body, immune cells are actively recruited to the biomaterials, which triggers a host inflammatory response and local tissue inflammation [4]. A good host inflammatory response can create a good immune microenvironment, which is an essential condition for bone tissue repair [5,6]. As the most important part of the host immune response, macrophages are the most important and studied. Macrophages can according to the shape function is divided into proinflammatory M1 macrophages and anti-inflammatory M2 macrophages. M1 macrophages can secrete a large number of pro-inflammatory factors, such as IL-1 and IL-6, which can stimulate stem cell migration and angiogenesis in the early stage [7]. However, continuous M1 macrophages can lead to chronic inflammation, which is not conducive to tissue repair. M2 macrophages can secrete bone morphogenetic protein 2 (BMP-2) and vascular endothelial growth factor (VEGF), promote bone formation and vascular growth [8–10].

The response of immune cells is regulated by a plethora of factors such as composition and topography of biomaterials [11,12]. The plasticity of macrophages to switch the phenotype in response to subtle changes opens the door to potential strategies in the development of bone

* Corresponding author. Department of Orthopedic Surgery, Xiangya Hospital Central South University, Changsha, China.
** Corresponding author. Department of Orthopedic Surgery, Xiangya Hospital Central South University, Changsha, China.
*** Corresponding author. Department of Orthopedic Surgery, Xiangya Hospital Central South University, Changsha, China.
E-mail addresses: liuwenbin1995@126.com (W. Liu), leipengfei@zju.edu.cn (P. Lei), xy_huyh@163.com (Y. Hu).

https://doi.org/10.1016/j.mtbio.2022.100340
Received 7 April 2022; Received in revised form 7 June 2022; Accepted 20 June 2022
Available online 25 June 2022

Table 1
Primer sequences.

Gene	Forward Primer sequences (5′–3′)	Reverse Primer sequences (5′–3′)
IL-1	GAAATGCCACCTTTTGACAGG	TGGATGCTCTCATCAGGACAG
IL-18	AGCAGTCCCAACTAAGCAGTA	CAGCCAGTAGAGGATGCTGA
IL-10	CTTACTGACTGGCATGAGGATCA	GCAGCTCTAGGAGCATGTGG
TNF-α	GGAACACGTCGTGGGATAATG	GGCAGACTTTGGATGCTTCTT
TGF-β	CTGGGTTGAGCAAGCCTACG	GGTCATTGCACATAACACGCT
VEGFA	ATGTCTACAGCGCAGCTACT	TCCGCATAATCTGCATGGTGA
Arg-1	CCAGATGTACCAGGATTCTC	AGCAGGTAGCTGAAGGTCTC
iNOS	CAGCTGGGCTGTACAAACCTT	CATTGGAAGTGAAGCGTTTCG

substitutes with osteoimmunomodulatory properties. Therefore, changes in the physical properties of the implant can change the phenotype of corresponding macrophages, release different cytokines, and create different immune microenvironment, ultimately eliciting different effects on bone dynamics [13].

In recent years, tantalum metal has been widely used in orthopedics and stomatology due to its excellent biological activity, biocompatibility, corrosion resistance and suitable mechanical properties [14]. Tantalum metal has good osteoinductivity, which is conducive to the proliferation and differentiation of osteoblasts [15–17]. It can form effective bone anchoring with human bone tissue and provide good initial stability. Therefore, porous tantalum implants are the most commonly used porous metal materials in hip arthroplasty and revision and have achieved satisfactory results [18]. Nowadays porous tantalum implants are made of tantalum micron particles [19]. Tantalum nanoparticles have been proved to have good bone induction. Both tantalum particles are used as adjuvants in biomaterials but little attention has been paid to their regulatory ability on macrophages around implants [14,20–22]. To clarify the response of tantalum particles to macrophages will help us better understand the influence of tantalum on the local immune microenvironment and the scope of clinical application.

In this study, we intended to explore the effects of different sizes of tantalum nanoparticles (nano tantalum and micron tantalum) on macrophage polarization to explore their effects on the immune microenvironment around the implant. First, we explored the effects of tantalum nanoparticles of different sizes on the gene expression and protein level of M1/M2-associated markers and cytokines under standard and inflammatory conditions. At the same time, the subcutaneous air pouch model was used to explore the regulation of immune microenvironment under the inflammatory conditions, and finally the specific mechanism was preliminarily explored.

2. Materials and methods

2.1. Materials

Tantalum nanoparticles (TaNPs) were purchased from Dk Nanotechnology (Beijing Dk Nano Technology Co, LTD, China). Morphology of TaNPs was observed by transmission electron microscope (HT7700, HITACHI, Japan). Tantalum micron particles (TaMPs) were purchased from Dk Nano Technology (Beijing Dk Nano Technology Co, LTD, China), and the morphology of TaMPs was observed by scanning electron microscope (MIRA4LMH, TESCAN, Czech). The particle size and Zeta-potential of TaNPs were analyzed by nanoparticle analyzer (SZ-100Z, HORIBA, Japan) in a deionized water mixture. TaNPs (50 mg) and TaMPs (50 mg) were sterilized by 60Co-γ Ray irradiation. The sterilized TaNPs were suspended in the complete medium, and sterile ultrasound was performed for 30 min to prepare 5 μg/mL and 5 mg/mL TaNPs suspensions respectively for the next step *in vivo* and *in vitro*.

2.2. In vitro studies

2.2.1. Cell culture

RAW 264.7 cell line was purchased from Procell Life

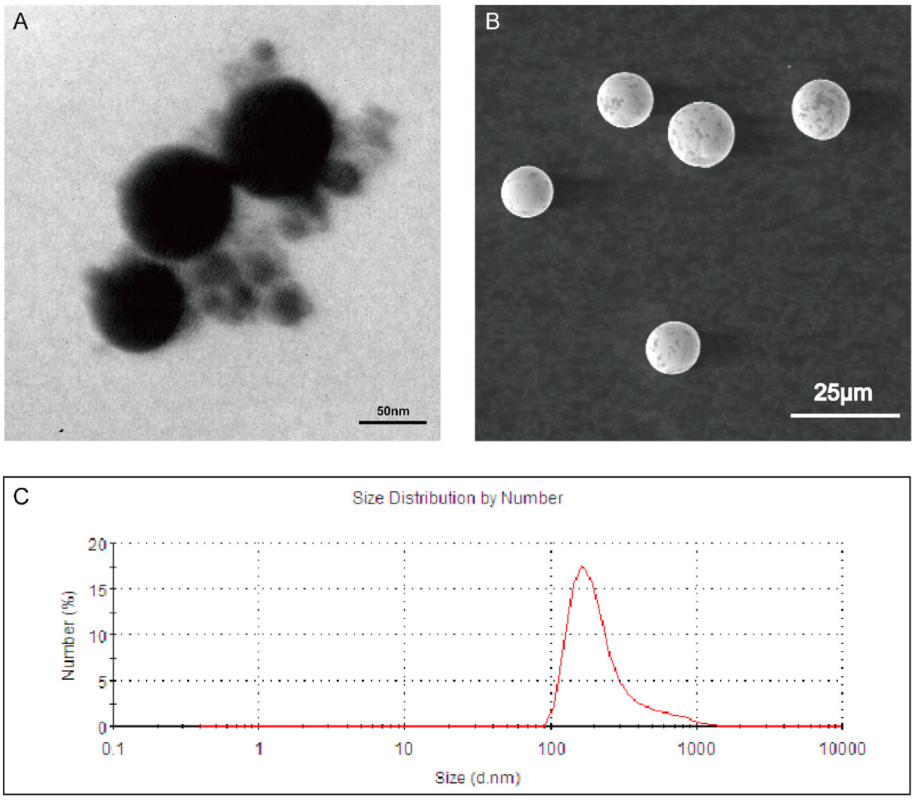

Fig. 1. General view and size of TaNPs and TaMPs. (A) TEM images of the TaNPs. (B) SEM images of the TaMPs. (C) Nanoparticle analyzer showing the particle size of TaNPs.

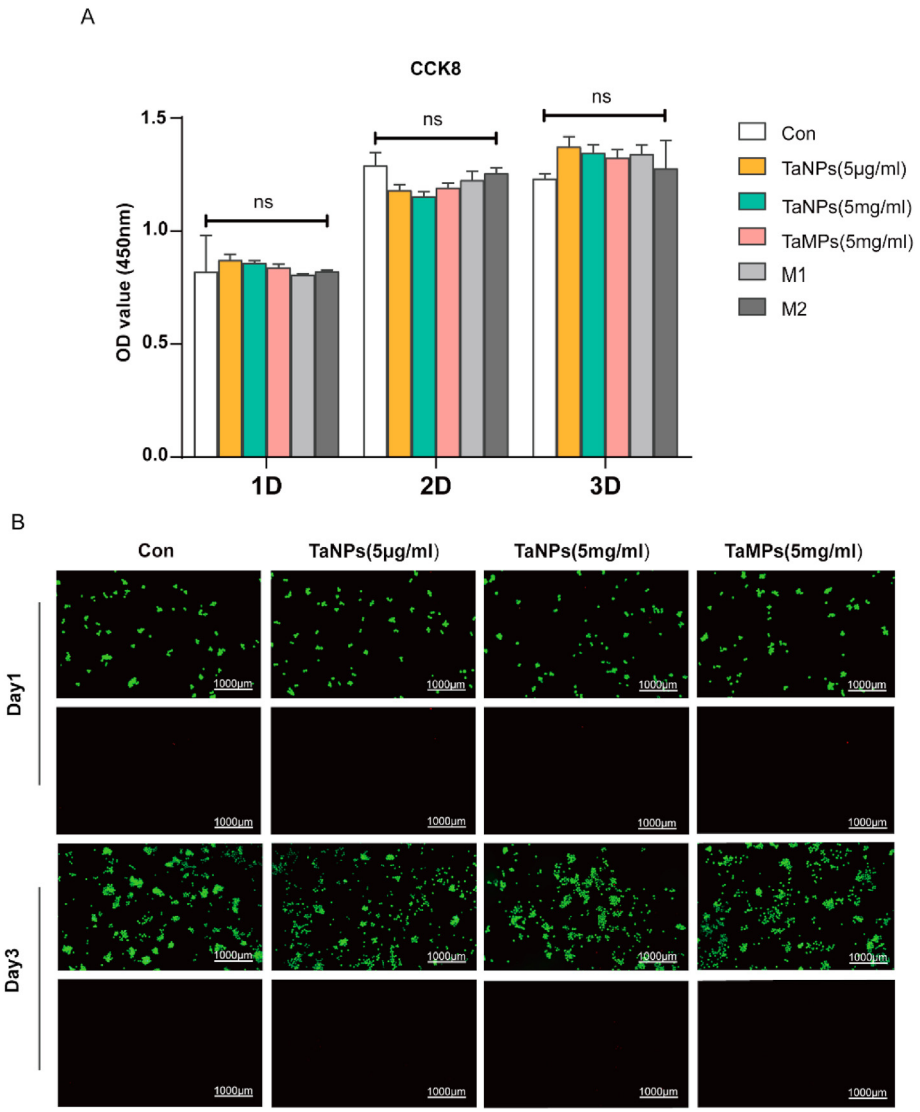

Fig. 2. Cytotoxicity and cell proliferation test. (A) Cell vitality of RAW cells with tantalum particles at 1, 2, and 3 days of culture, detected by CCK-8. No significant difference was found between various groups (B) Live/dead assay of RAW cells. Scale bar = 1000 μm. (*P < 0.05, **P < 0.01, ***P < 0.001).

Science&Technology C, Ltd. (CL-0190, Procell, China). Cells were cultured in RAW 264.7 specialty medium (Procell, China) at 37 °C and 5% CO2. The medium contained 10% fetal bovine serum (FBS) and 1% penicillin/streptomycin (HyClone, Logan, USA). Consistent with previous literature reports, *E. coli* saccharide (LPS) and interferon-γ (IFN-γ) were used as M1 macrophage stimulating factors, and interleukin-4 (IL-4) as M2 macrophage stimulating factors [23].

2.2.2. Cytotoxicity and cell proliferation

To study the biocompatibility of tantalum particles, RAW 264.7 cells were co-cultured with TaNPs (5 μg/mL), TaNPs (5 mg/mL) and TaMPs (5 mg/mL) respectively. RAW 264.7 cells cultured without tantalum particles were used as a control group (Con). The cells cultured with LPS (100 ng/mL) and IFN-γ (20 ng/mL) were taken as the M1 group, and the cells cultured with IL-4 (20 ng/mL) were taken as M2 group [24]. The cell viability of RAW 264.7 cells was evaluated by CCK-8 kit (New Cell & Molecular Biotech Co, Ltd, China). Briefly, the cells were seeded in 96-well plates (Guangzhou Jet Bio-Filtration Co. Ltd) at a density of 5.0 × 10^3 cells/well and incubated overnight. Then 100 μL 10% CCK-8 solution was added to each well and cells were incubated for 2 h after 1, 2, and 3 days. The absorbance was detected with a microplate reader at 450 nm wavelength. RAW 264.7 cells were inoculated at a density of 1 × 10^5 cells/well in a laser confocal culture dish for 12 h. After 1 day and 3 days, live/dead staining was performed. Photographs were taken using a fluorescence microscope.

2.2.3. Cell morphology

The morphology of macrophages was observed by F-actin staining. RAW 264.7 cells were treated according to 2.2.2 and fixed with 4% paraformaldehyde for 15 min. After fixation, 0.1% TritonX-100 was added to break the membrane at room temperature for 10min. Following the incubation, the plates were stained with TRITC Phalloidin which was prepared by 1% BSA and incubated for 1 h. After washing with PBS for 3 times, the plates were stained with 4', 6-diamidino-2-phenylindole (DAPI, Solarbio, China) for 10 min, and plates were washed with PBS. The plates were observed and captured by laser confocal microscopy.

2.2.4. RT-qPCR

Cells were cultured and grouped as shown in 2.2.2. After 12 h and 24 h of intervention, respectively, cells were washed by PBS, and Trizol was used to extract total RNA. cDNA was prepared by reverse transcription using Prime Script RT Reagent Kit (Takara Bio, Otsu, Japan). Real-time qPCR (ABI ViiA7, Thermo Fisher Scientific, Waltham, USA) was used to analyze the M1 phenotype (IL-1, IL-18, TNF-α, iNOS) and M2

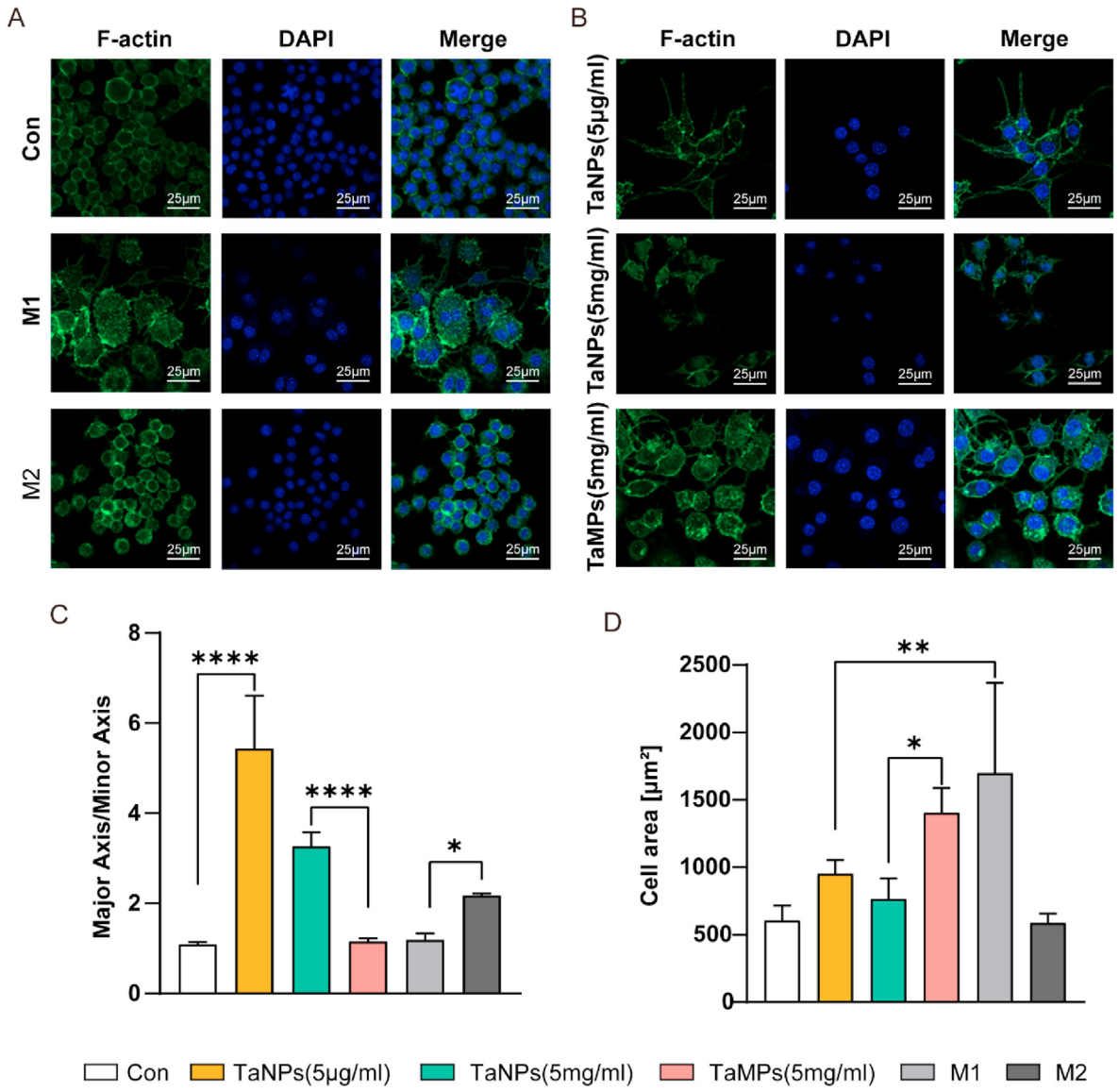

Fig. 3. Effect of tantalum particles on cell morphology of macrophages. Cells were stained for F-actin (green), nuclei (blue) (A, B). (C) Statistical analysis of major axis and minor axis ratio of macrophages. (D) Statistical analysis of surface area of macrophages. Scale bar = 25 μm. (*P < 0.05, **P < 0.01, ***P < 0.001, ****P < 0.0001). (For interpretation of the references to colour in this figure legend, the reader is referred to the Web version of this article.)

phenotype (IL-10, Arg-1, TGF-β, VEGF) related genes (primers were listed in Table 1). 2-△△Ct was used to quantify the relative levels of different mRNA expressions. All samples are normalized to GAPDH.

2.2.5. Flow cytometry

Cells were digested by trypsin, and collected and resuspended with PBS for flow cytometry, after treatment as 2.2.2 for 12 h. Then incubate with F4/80 and CD86 (Univ, CHINA, #565410, #560582, dilution ratio:1:50) on ice for 30 min, add 1 mL PBS for washing, and centrifugation. The supernatant was discarded, the membrane was fixed and broken overnight at 4 °C. After cleaning, the supernatant was discarded, CD206 was added and incubated on ice for another 40 min. After cleaning, flow cytometry (BD FACSCalibur, BD Bioscience, New York, USA) was used for analysis. The data was analyzed using FlowJo V10 software.

2.2.6. Immunofluorescence

Immunofluorescence staining was performed with Arginase 1 (Arg-1) (AF20179 , AiFang Biological) and inducible nitric oxide synthase (iNOS) (Abcam, USA). Cells were treated as 2.2.2. After removing the medium, the cells were washed carefully with PBS to prevent shedding, and then fixed with 4% paraformaldehyde for 15 min. After fixation, 0.1% TritonX-100 was added to break the membrane at room temperature for 10 min, and then sealed with 5% BSA for 1 h to remove the nonspecific antigen. Add the primary antibody diluted by 5% BSA to the perforated plate, and place it on a 4 °C overnight. After incubation, the secondary antibody was added to the plate well. Then the perforated plate was incubated at room temperature for 1 h. At last, the nuclei were stained with re-stained DAPI after completion in 1 min. Cells were observed and imaged by laser confocal microscopy.

2.2.7. Reactive oxygen species assay

Cells were treated as 2.2.2. Firstly, DCFH-D was diluted with a serum-free medium at 1:1000 to achieve a final concentration of 10 mM. Then the cell culture medium was removed and an appropriate volume of diluted DCFH-DA was added. 1 mL of diluted DCFH-DA were added to each well of the six-well plate. Incubating for 20 min in the cell culture box at 37 °C. The cells were washed three times with a serum-free cell culture medium and imaged by laser confocal microscopy.

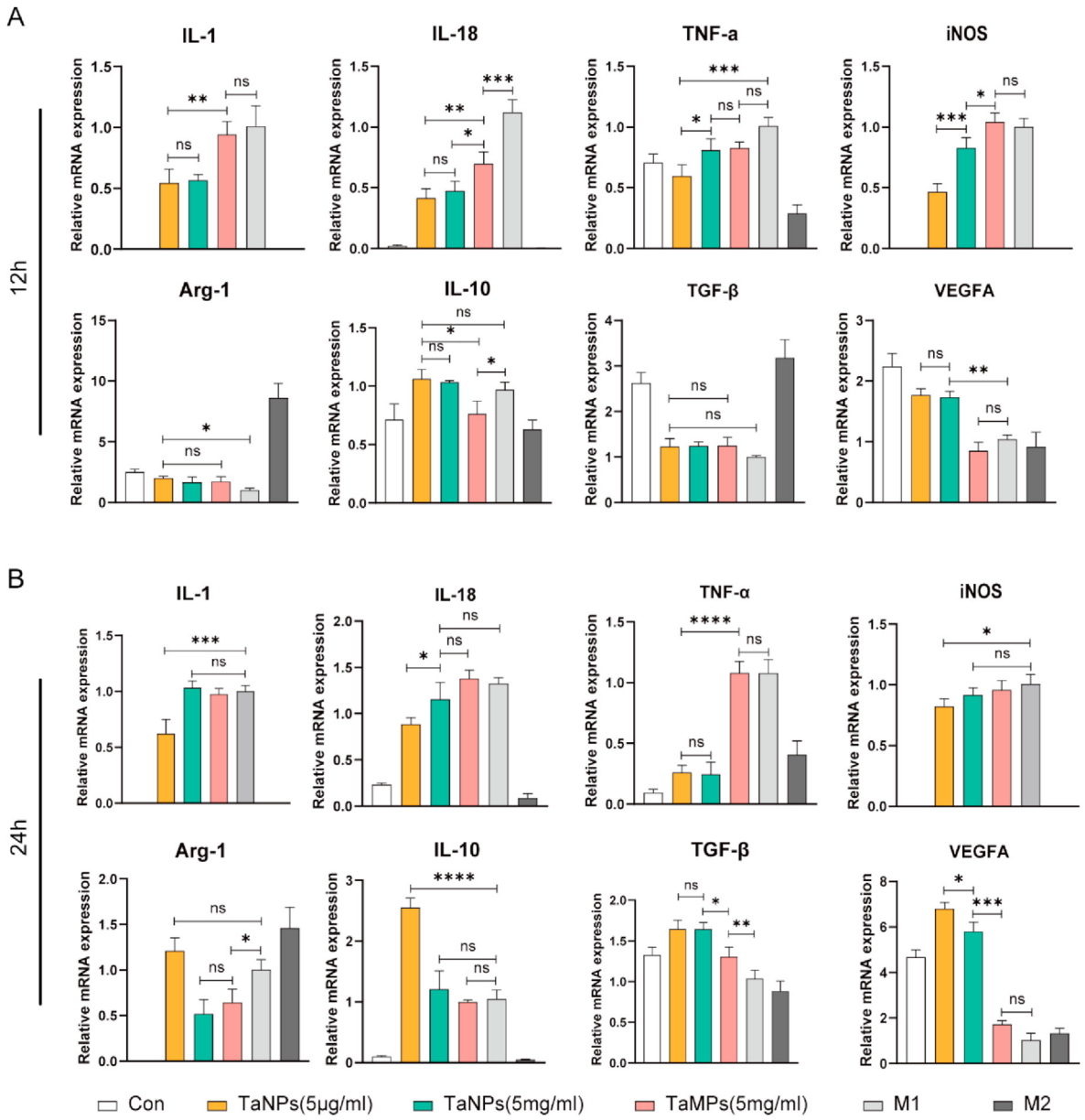

Fig. 4. TaNPs inhibited the LPS-induced inflammatory response of macrophages and promoted the macrophage phenotype to switch from M1 to M2. (A) Real-time PCR analysis of the gene expression of the M1-related IL-1, IL-18, TNF-α, and iNOS and the M2-related Arg-1, IL-10, TGF-βand VEGFA after 12 h intervention. (B) Real-time PCR analysis of gene expression of the M1-related IL-1, IL-18, TNF-α and iNOS and the M2-related Arg-1, IL-10, TGF-β and VEGFA after 24 h intervention. (*P < 0.05, **P < 0.01, ***P < 0.001, ****P < 0.0001).

2.2.8. *Proteome Profiler Mouse XL Cytokine Array*

Cells were treated as 2.2.2. After discarding the supernatant, cells were washed with PBS for three times. Then cell culture medium without cytokines was added and cells were incubated overnight. The supernatant was assayed immediately after collection and centrifugation. Exposure was carried out by chemiluminescence instrument, and Assay immediately, then image-J was used to analyze the experimental results.

2.3. *In vivo experiment*

The animal experiment program was approved by the Biomedical Research Ethics Committee of Central South University (License Number: 2022020556). Twenty C57 mice (6–8 weeks of age) were randomly divided into 5 groups: (1) blank (control group), (2) 5 μg/mL TaNPs, (3) 5 mg/mL TaNPs, (4) 5 mg/mL TaMPs, and (5) 100 ng/mL LPS and 20 ng/mL IFN-γ. After pentobarbital sodium anesthesia, 2 mL sterile air was injected subcutaneously into the back of the mice, and 1 mL sterile air was supplemented on the 3rd and 7th day, respectively [25]. After the balloon was stabilized, liquid and tantalum particles were injected into the back balloon of the mice according to the above groups, and the mice were sacrificed on the 4th and 7th day after implantation to obtain the balloon tissue.

The pouch tissue was fixed with paraformaldehyde for 1 week, and local inflammatory response was evaluated. Paraformaldehyde fixed paraffin-embedded scaffold specimens were cut into continuous sections (7 μm). Then the sections were dewaxed and fixed, and the fixed sections were sealed with serum for 30 mins, then incubated overnight with primary antibody. After being cleaned for 3 times, the sections were incubated for 50 mins with secondary antibody at room temperature. The nuclei were stained with DAPI, and incubated for 10 mins. Finally, the sections were sealed for observation.

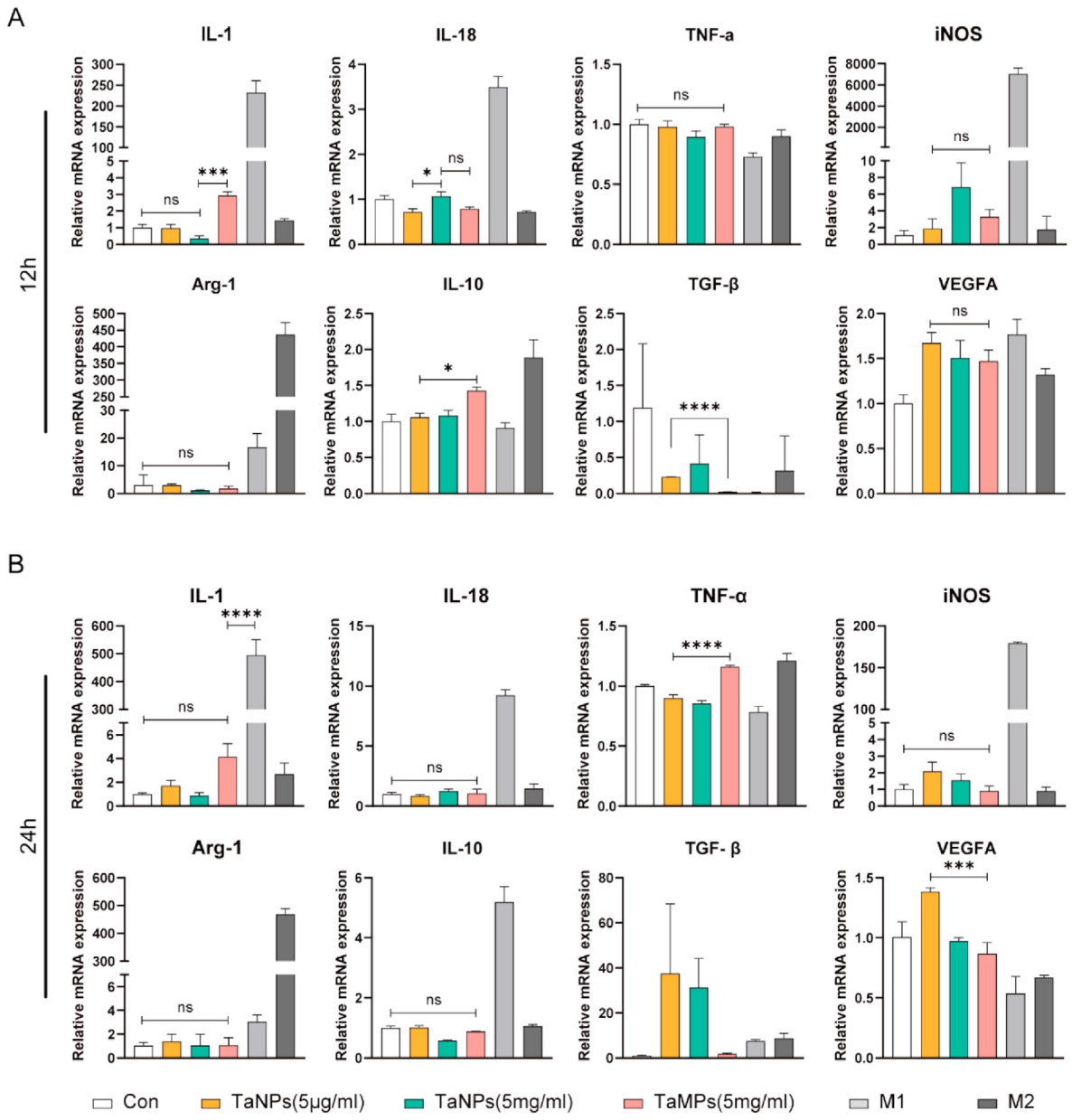

Fig. 5. The effects of TaNPs and TaMPs without LPS and IFN-γ intervention on inflammatory factors in macrophage RNA levels. (A) Real-time PCR analysis of the gene expression of the M1-related IL-1, IL-18, TNF-α, and iNOS and the M2-related Arg-1, IL-10, TGF-βand VEGFA after 12 h intervention. (B) Real-time PCR analysis of the gene expression of the M1-related IL-1, IL-18, TNF-α, and iNOS, and the M2-related Arg-1, IL-10, TGF-β and VEGFA after 24 h intervention. (*P < 0.05, **P < 0.01, ***P < 0.001, ****P < 0.0001).

2.4. Statistical analysis

Each experiment was repeated three times to obtain approximate results. The data were expressed as mean standard deviation. Data were compared within groups by student T-test and between groups by one-way ANOVA. When $P < 0.05$, the results were considered statistically significant. All analyses were performed using GraphPad Prism 8.0 (GraphPad Software, USA).

3. Results

3.1. Characterization of TaNPs and TaMPs

TaNPs and TaMPs were uniformly spherical under SEM and TEM. The particle size of TaNPs was about 100 ± 20 nm (Fig. 1A), and the particle size of TaMPs was about 14 ± 1.7 μm. Statistical figure of tantalum microparticle size is shown in Fig.S1. The suspended particle size of TaNPs in solution is 133 ± 6.3 nm, and the Zeta potential is 20.1 ± 4.8 mV.

3.2. Cytotoxicity of tantalum particles

First, the CCK-8 assay was applied to detect the cell viability and proliferation of RAW cells after adding tantalum particles. As shown in Figs. 2A, 1 and 2, and 3 days after the intervention, there was no significant difference among the groups. Therefore, in general, TaNPs and TaMPs do not negatively affect cell proliferation. Then, the effects of two tantalum particles on the proliferation and cell morphology of RAW cells were detected by live/dead staining (Fig. 2B).

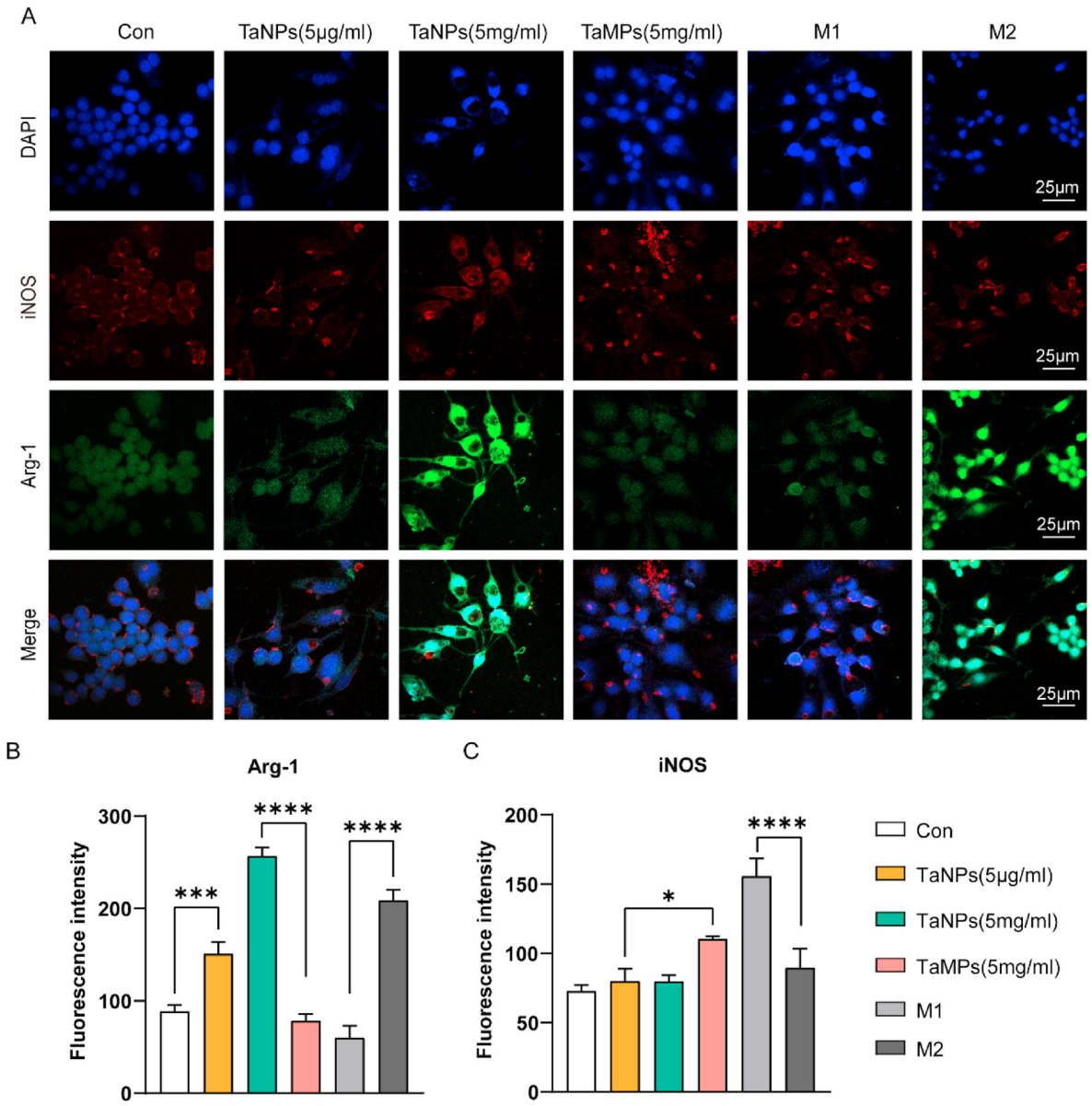

Fig. 6. Effect of Tantalum particles on macrophage phenotypes under inflammatory conditions with LPS and IFN-γ intervention. (A)Cells were stained for iNOS (red), Arg-1 (green), nuclei (blue). (B) Statistical analysis of the fluorescence intensity of Arg-1. (C) Statistical analysis of the fluorescence intensity of iNOS. Scale bar = 25 μm. (*P < 0.05, **P < 0.01, ***P < 0.001, ****P < 0.0001). (For interpretation of the references to colour in this figure legend, the reader is referred to the Web version of this article.)

3.3. Morphology of macrophages

Macrophages can be induced into M0, M1, and M2 phenotypes under different culture conditions, and each phenotype of macrophages have specific morphologies [26]. Therefore, we can preliminarily judge the influence of different intervention factors on the phenotype of macrophages by observing the morphology of macrophages. In this experiment (Fig. 3A & B), we found that RAW in the control group was small and round with a large number of cells clustered and distributed in clusters, which were mostly typical M0 phenotype cells [27]. The cell volume slightly increased in both groups with TaNPs, which showed a spindle morphology (Fig. 3C). A small number of cells clustered and distributed, showing approximately M2 phenotype [28]. The cell volume of TaMPs and M1 group significantly increased with more pseudopodia, and the cell distribution was relatively dispersed (Fig. 3D). M2 group was typical M2 macrophages with small volume and shuttle type volume elongation. Therefore, under inflammatory conditions, the morphology of macrophages after TaNPs intervention is closer to the M2 phenotype, while the morphology of macrophages after TaMPs intervention is closer to the M1 phenotype.

3.4. Immunomodulation of macrophages by tantalum particles

To study the effects of different tantalum particle sizes on gene expression in macrophages under LPS-activated inflammatory conditions, RT-qPCR was used to analyze the expression of inflammatory genes in macrophages. As is shown in Fig. 4, TaNPs (5 μg/mL) inhibited M1-related genes (IL-1, IL-18, iNOS, TNF-α) and promoted M2-related genes (Arg-1, IL-10, TGF-β1, VEGFA) expression compared with M1-positive control group [29]. At the same time, the regulation of macrophage polarization was more after TaNPs and RAW were co-cultured for 24 h, compared with the results of co-culture for 12 h. TaMPs down-regulated the expression of IL-18 at 12 h and up-regulated the expression of TGF-β1 at 24 h. However, from the overall expression of

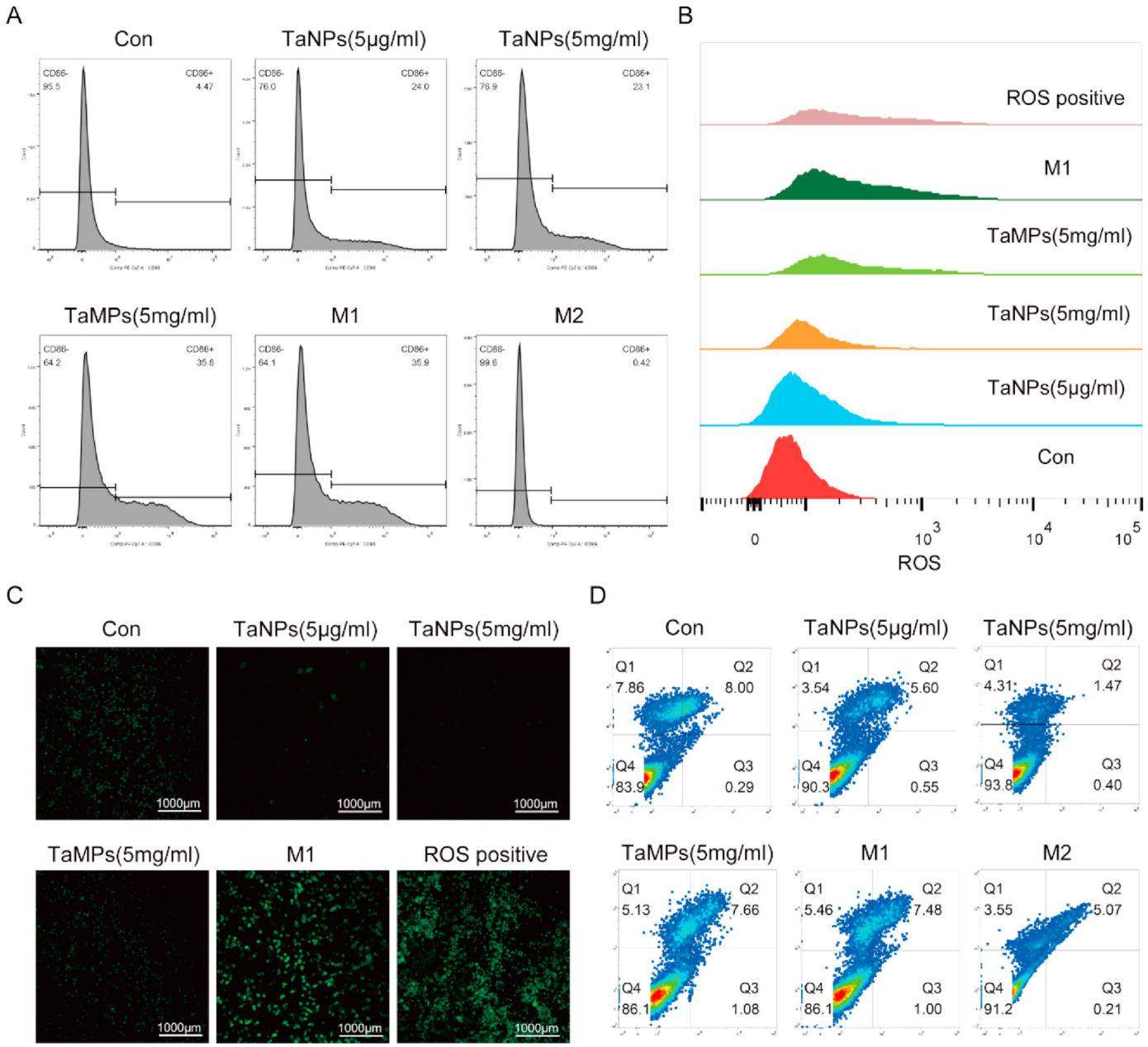

Fig. 7. (A) Flow cytometry analysis of the M1-related marker CD86 on RAW 264.7. (B) Flow Cytometry Analysis of ROS Content in RAW Cells (C) Observation of ROS content in RAW by confocal microscopy (D) The effect of TaNPs and TaMPs on the apoptosis of macrophages under inflammatory conditions, detected by Annexin V-FITC/PI apoptosis detection kit.

genes at the two-time points, there was no clear evidence that TaMPs are able affect M1 and M2-related genes. At the same time, to explore the effect of macrophages on TaNPs and TaMPs without LPS activation, RT-qPCR was used to analyze the expression of inflammatory genes in macrophages again, and the results (Fig. 5) showed that in the absence of LPS and IFN-γ intervention, the effect of TaNPs and TaMPs on inflammatory factors in macrophages was not obvious at RNA level.

To further explore the changes in macrophage at protein level, immunofluorescence staining was used to detect the changes of Arg-1 and iNOS in macrophages. As shown in Fig. 6, the fluorescence intensity of Arg-1 in TaNPs group and M2 group was higher than that in the other groups, and TaNPs group (5 mg/mL) had the strongest fluorescence intensity. At the same time, we also observed that the iNOS fluorescence intensity of TaMPs group and M1 group were higher than other groups, and the iNOS protein fluorescence intensity of TaNPs (5 μg/mL) and Con group were lower. In conclusion, TaNPs (5 μg/mL) and TaMPs (5 mg/mL) promoted the expression of M2-related protein (Arg-1) and inhibited the expression of m1-related protein (iNOS) (Fig. 6A). This was also supported by the fluorescence intensity statistics of Arg-1 and iNOS (Fig. 6B & C). TaMPs have no specific effect on the phenotype of macrophages under inflammatory conditions at protein level.

Flow cytometry was used to detect the expression of CD86 (M1 phenotype macrophage marker) and determine the changes of macrophage phenotype. As shown in Fig. 7A, in the inflammatory environment induced by LPS and IFN-γ, the positive rates of CD86 in the two groups of macrophages added with TaNPs were 24.0% and 23.1%, respectively, and the positive rates of CD86 in the TaMPs and M1 control group were 35.8% and 35.9%, respectively. According to the analysis of the positive rate of CD86, TaNPs inhibited the up-regulation of CD86 in the inflammatory environment to a certain extent, but such a phenomenon was not observed in the TaMPs group at both concentrations. At the same time, flow cytometry was also used to detect the expression of CD206 (M2

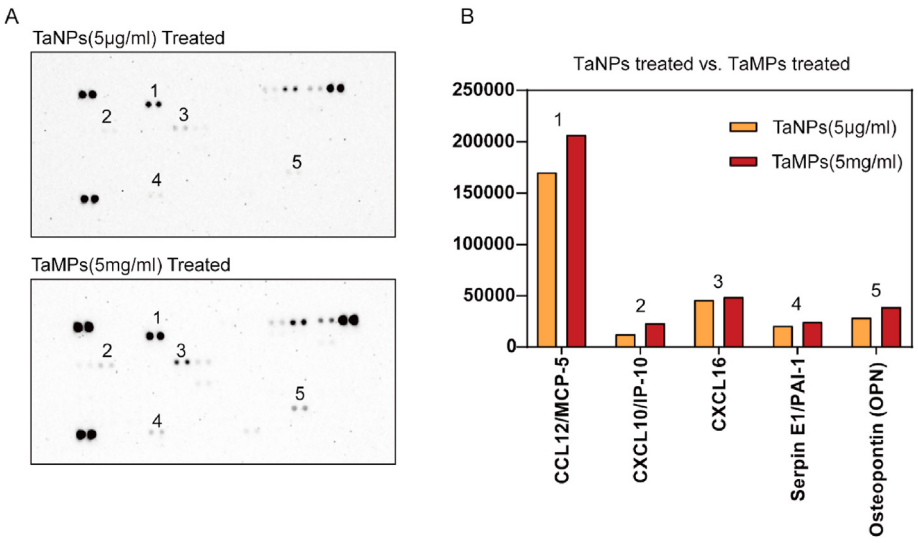

Fig. 8. Detection of cytokines secreted from RAW 264.7 cell line. (A)The cytokines secreted by RAW under different culture conditions were detected by Proteome Profiler Mouse XL Cytokine Array. (B) The points in figure A were statistically analyzed according to the grayscale.

phenotype macrophage marker) [30]. However, due to the low expression level of CD206 in the RAW264.7 cell line, the expression of CD206 was not significantly changed under the intervention of the two tantalum particles.

3.5. Effects of tantalum particles on ROS in macrophages

To explore the possible mechanism underlying the above phenomena, flow cytometry and ROS kits were applied to detect the level of reactive oxygen species in macrophages in each group under the inflammatory environment. The results (Fig. 7B & C) showed that compared with the M1 positive control group and ROS positive control group, TaNPs (5 μg/mL) and TaNPs (5 mg/mL) groups had lower fluorescence intensity. The fluorescence intensity of TaMPs group was slightly lower than the M1 control group and positive control group. The results show that TaNPs significantly reduced intracellular reactive oxygen species content, and TaMPs group had a certain effect on reducing the intracellular oxygen content. Reactive oxygen content and TaMPs group had a certain effect on reducing the intracellular oxygen content. Finally, we used the transfer kit to detect the effects of tantalum nanoparticles and tantalum microparticles on macrophages. The results (Fig. 7D) showed that the above two particles had no significant effect on the cell cycle.

3.6. Effects on macrophage cytokines

Cytokine secreted from macrophages under TaNPs and TaMPs intervention was detected using Proteome Profiler Mouse XL Cytokine Array [31]. The results (Fig. 8) are shown in Fig. 8D, it was observed that macrophages secreted fewer CCL12, CXCL10, CXCL16, and Serpin E1 under TaNPs intervention, which are all pro-inflammatory related cytokines. At the same time, it was also observed that under the intervention of TaNPs and TaMPs, macrophages secreted Osteopontin (OPN), and TaMPs had a stronger effect on promoting the secretion of OPN.

3.7. Effects of tantalum particles on inflammation in vivo

Mouse air pouch models were used to explore the effects of TaNPs and TaMPs on inflammation under *in vivo* conditions. The air pouch sections were subjected to H&E staining and histochemical fluorescence, and the results were shown in Fig. 9. Compared with other groups, the air pouch injected with LPS had stronger iNOS fluorescence on the 4th and 7th days, and the balloon wall under TaNPs and TaMPs intervention had stronger Arg-1 fluorescence at 4 days and 7 days. This indicates that both TaNPs and TaMPs can regulate inflammation to a certain extent under *in vivo* conditions, that is, have a certain anti-inflammatory effect. There was no significant difference in H&E of balloon wall sections.

4. Discussion

Biomaterials rapidly recruit immune cells and induce cytokine secretion after implantation. Among them, macrophages not only release a large number of inflammatory factors but also play an important role in wound healing and tissue repair [32,33]. Due to this dual effect, the polarization of macrophages around the biomaterial either brings the success of transplantation or leads to chronic inflammation and graft rejection [34,35]. In this study, RAW 264.7 cells were used to study the response of macrophages to tantalum particles of different sizes and concentrations under inflammatory conditions. LPS was used to activate RAW264.7 cells, a commonly used macrophage-type cell line, simulating an inflammatory environment around the prosthesis and make the cells respond more sensitively to external stimuli [36]. The proliferation and morphology evaluation of macrophages is an important means to evaluate the development degree and activation stage of inflammation [37]. Results showed that both TaNPs and TaMPs had no effects on the proliferation of RAW and did not exhibit cytotoxicity. In other words, within a certain concentration range, even if macrophages engulf tantalum particles, the cells remain intact. This constitutes a prerequisite for further research on the effects of tantalum particles on macrophages.

The morphology of macrophages is closely related to their polarization state [38]. M1 phenotype macrophages are usually round with large cell surface area and more pseudopodia, while M2 phenotype macrophages are more elongated in shape with small cell surface area. In addition, after LPS induction, the proliferation of M1 phenotype macrophages was enhanced and the distribution was more dispersed. Our results showed that RAW 264.7 with TaNPs was more similar to M2 phenotype in morphology in LPS-induced inflammatory environment, while that with TaMPs were more similar to M1 phenotype in cell morphology. In other words, TaNPs promoted the morphological polarization of LPS-activated macrophages toward M2-like phenotype, and the polarization of macrophages after TaMPs treatment was M1-like phenotype, which was consistent with the polarization of macrophages induced by LPS and IFN-γ. That is to say, from the perspective of cell morphology, TaNPs reversed LPS-induced changes in macrophages and showed a better phenotypic conversion ability in macrophages.

At the same time, it must be considered that the morphological changes of macrophages not only depend on the intervention of

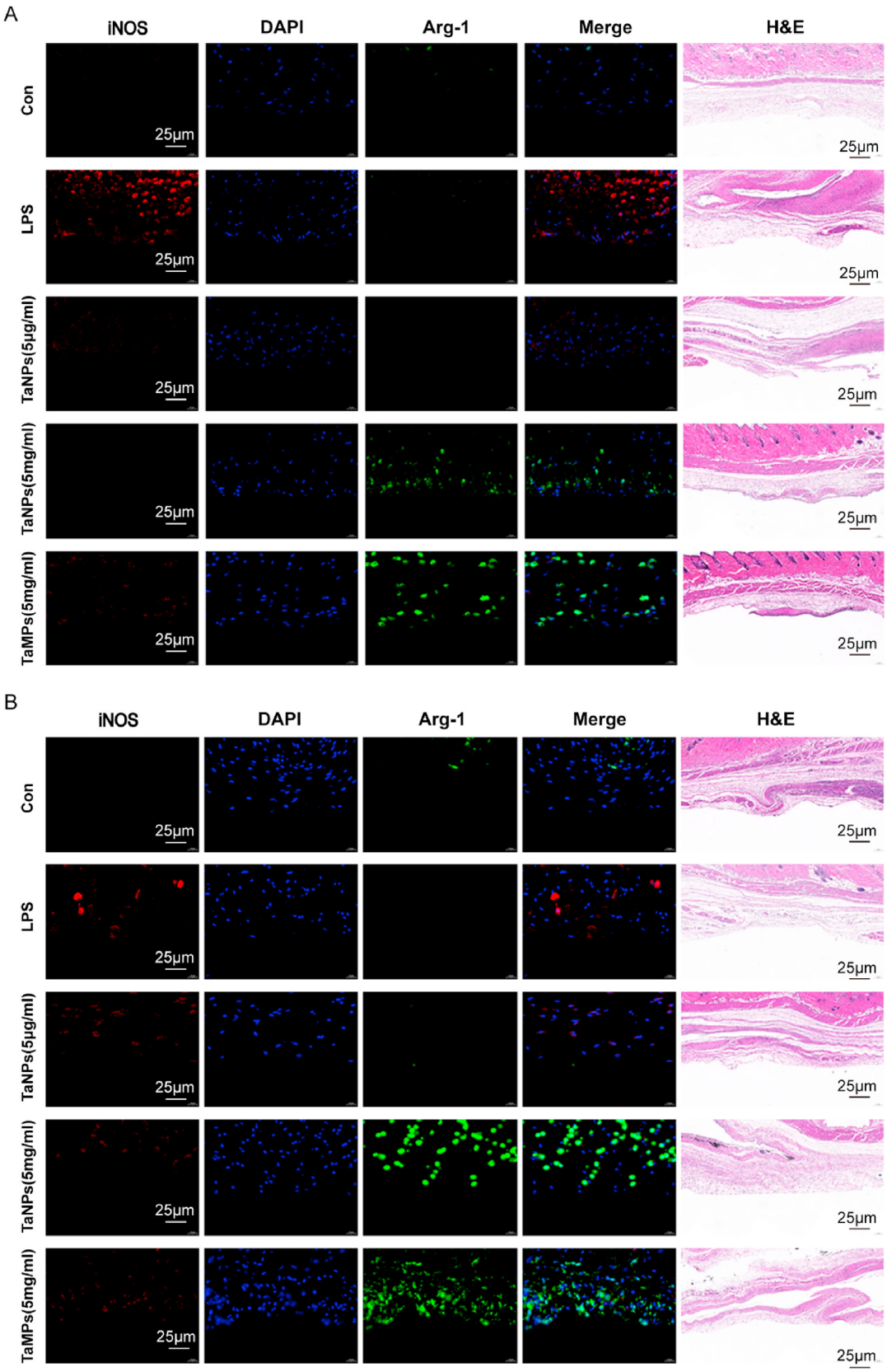

Fig. 9. In the subcutaneous air pouch model, TaNPs showed good immunomodulatory potential in an inflammatory environment. Figure (A) is HE staining and immunofluorescence of mouse air pouch section on the 4th day, and (B) is HE staining and immunofluorescence of mouse air pouch section on the 7th day. Scale bar = 25 μm.

exogenous stimulus factors but also can be affected by the cytokines produced by themselves. Therefore, detection of cytokine secretion can more accurately indicate the polarization of macrophages than morphological observation. Therefore, we used RT-qPCR to detect the gene expression levels of related cytokines in macrophages [39,40]. Macrophages with the M1 phenotype usually secrete pro-inflammatory factors, including (IL-1, IL-18, TNF-α). Cytokines commonly secreted by the M2 phenotype include IL-10, TGF-β, and VEGFA [41]. The results showed that TaNPs (5 μg/mL) inhibited the expression of M1-phenotypic related genes (IL-1, IL-18, TNF-α) and promoted the expression of M2-phenotypic related genes (IL-10, TGF-β, VEGFA) in the inflammatory environment compared with the M1-positive control group. At the same time, we also detected the abundance of Arg-1 and iNOS in macrophages by immunofluorescence method, and the results showed that TaNPs (5 μg/mL) and TaMPs (5 mg/mL) promoted the expression of Arg-1 and inhibited the expression of iNOS (Fig. 7). TaMPs showed no effect on macrophage phenotype at protein level under inflammatory conditions. These results suggest that TaNPs have different effects on macrophage activation compared with TaMPs, and we found some evidence about this at both gene expression level and protein level. That is to say, TaNPs regulate the function of activated macrophages and makes them polarized toward the promotion of tissue repair, while TaMPs does not show obvious pro-inflammatory effects on LPS-activated macrophages, nor does it show obvious anti-inflammatory effects. The effect of promoting its polarization in the direction of tissue repair has no obvious effect on macrophages in an inflammatory environment. Meanwhile, RT-qPCR examined the effects of TaNPs and TaMPs without LPS and IFN-γ intervention on inflammatory factors in macrophage RNA levels. The effect of endogenous inflammation-related mRNA levels was not statistically significant compared with the control group.

Next, to more directly determine the polarization typing of macrophages, flow cytometry was used to detect the expression rate of signature proteins on RAW 264.7. The obtained trend was consistent with RT-qPCR and immunofluorescence. TaNPs at both concentrations inhibited CD86 upregulation in the inflammatory environment to a certain extent, that is to say, TaNPs inhibited macrophage polarization to the M1 phenotype. However, due to the low expression level of M2 phenotypic marker protein in the RAW 264.7 cell line, there was no direct evidence to reflect the change in the proportion of M2 phenotypic macrophages. At the same time, TaMPs showed no effect on macrophage phenotype under inflammatory conditions. Subsequently, the Proteome Profiler Mouse XL Cytokine Array was used to detect cytokines secreted by macrophages, and the results showed that TaNPs had a stronger inhibitory effect on the secretion of inflammatory cytokines under inflammatory conditions [42]. The air pouch model showed that both TaNPs and TaMPs inhibited the expression of iNOS under LPS intervention. This indicates that both kinds of tantalum particles have certain anti-inflammatory effects *in vivo*. At the same time, TaNPs (5 mg/mL) and TaMPs (5 mg/mL) both promoted the expression of Arg-1, which may be related to the fibrosis of the airbag wall wrapping tantalum particles, and the specific mechanism remains to be further explored.

According to literature review, ROS is crucial to the induction and maintenance of polarization of M1-type macrophages [43]. Several studies have reported the role of ROS in activating nuclear factor kappa-B (NF-κB) and P38 mitogen-activated protein kinase (P38MAPK) signaling pathways that promote the expression of pro-inflammatory genes in macrophages [44,45]. One possible mechanism is ROS activation of NOX and SOD, which leads to increased production of H2O2 under Toll-like receptor 4 (TLR4) stimulation. H2O2 as a consequence diffused from the phagosome, leading to dissociation of the apoptotic signal-regulated kinase (ASK1) inhibitor thioredoxin from the ASK1-TrX complex, inducing ASK1 phosphorylation and activation of downstream P38MAPK. In addition, ROS enhances phosphorylation of the NFκB inhibitor IκB, leading to activation of the NFκB pathway. In addition, ROS is a prerequisite for the activation of NOD-like receptor protein 3 inflammasome (NLRP3) in inflammasome, which leads to the high secretion of IL-1β and IL-18, the inflammatory environment that maintains the microenvironment, and the M1 phenotype polarization of macrophages [46]. Given this, we speculate that the ability of TaNPs to regulate the phenotypic transformation of macrophages is related to intracellular ROS level. So, we detected the changes of ROS levels in macrophages in the inflammatory environment by ROS Kits. The results showed that the addition of TaNPs decreased the ROS level incells. To explore the effect of TaNPs and TaMPs on macrophages apoptosis under inflammatory conditions, the cells underwent flow cytometry with Annexin V-FITC/PI apoptosis detection kit [47]. Apoptosis was not significantly affected. This suggests that TaNPs may indeed change the polarization phenotype of macrophages by reducing intracellular ROS levels and regulating subsequent pathways. We found that macrophages can phagocytose TaNPs by transmission electron microscopy (Fig.S2). The mechanism by which TaNPs affect macrophage polarization is complex, but we believe that TaNPs play an important role in NFκB and MAPK signaling pathways by reducing ROS expression. Compared with TaMPs, the anti-inflammatory effect of TaNPs provides room for imagination for the application of nano tantalum particles.

5. Conclusion

In conclusion, this study, for the first time, investigated the differential effects of nano- and micro-scale tantalum particles in the immunomodulatory process. We demonstrated that TaNPs can modulate the inflammatory response, macrophage polarization, and cytokine production in an inflammatory environment, thereby improving the inflammatory microenvironment around the tissue. TaMPs are inert in an inflammatory environment, that is, they have no significant effect on the process of inflammation. This study also preliminarily illustrated that ROS may be the key factor of TaNPs regulation in immune microenvironment. These findings suggest the potential application of TaNPs in tissue engineering and related inflammation therapy.

Credit author statement

Yan Sun: Conceptualization, Methodology, Formal analysis, Investigation, Data Curation, Writing - Original Draft, Visualization. **Tuozhou Liu**: Investigation, Data Curation. **Hongkun Hu, Zixuan Xiong** and **Kai Zhang** contributed to the data analyses in this experiment. **Xi He:** Funding acquisition**, Wenbin Liu**: Conceptualization, Methodology, Formal analysis, Investigation, Data Curation, Writing - Original Draft, Visualization. **Hu Yihe**: Writing - Review & Editing, Supervision, Project administration, Funding acquisition. **Pengfei Lei**: Writing - Review & Editing, Supervision, Project administration, Funding acquisition.

Declaration of competing interest

The authors declare that they have no known competing financial interests or personal relationships that could have appeared to influence the work reported in this paper.

Acknowledgements

This study was supported by the Natural Science Foundation of China (Grant Nos. 82002277 and 81672656), Natural Science Foundation of Hunan Province, China (Grant Nos. 2018JJ3844 and 2019JJ40499), the Scientific Research Project of Health and Family Planning Commission of Hunan Province, China (Grant No. B2019188), the Key Research and Development program of Hunan Province (Grant Nos. 2020SK2008 and 2021GK2012), the Major Science and Technology projects of Changsha City (Grant No. kh2003016). National Key Research and Development project (2016YFC1100605 and 2018YFB1105504). Clinical research fund of National Clinical Research Center for Geriatric Disorders (Xiangya Hospital, Grant No. 2020LNJJ15).

Appendix A. Supplementary data

Supplementary data to this article can be found online at https://doi.org/10.1016/j.mtbio.2022.100340.

References

[1] L. Partridge, J. Deelen, P.E. Slagboom, Facing up to the global challenges of ageing, Nature 561 (7721) (2018) 45–56.
[2] X. Gao, L. Li, X. Cai, Q. Huang, J. Xiao, Y. Cheng, Targeting nanoparticles for diagnosis and therapy of bone tumors: opportunities and challenges, Biomaterials 265 (2021), 120404.
[3] S.B. Goodman, Z. Yao, M. Keeney, F. Yang, The future of biologic coatings for orthopaedic implants, Biomaterials 34 (13) (2013) 3174–3183.
[4] L.C. Borish, J.W. Steinke, 2. Cytokines and chemokines, J. Allergy Clin. Immunol. 111 (2 Suppl) (2003) S460–S475.
[5] D. Lopes, C. Martins-Cruz, M.B. Oliveira, J.F. Mano, Bone physiology as inspiration for tissue regenerative therapies, Biomaterials 185 (2018) 240–275.
[6] T. Sun, C.H.T. Kwong, C. Gao, J. Wei, L. Yue, J. Zhang, R.D. Ye, R. Wang, Amelioration of ulcerative colitis via inflammatory regulation by macrophage-biomimetic nanomedicine, Theranostics 10 (22) (2020) 10106–10119.
[7] E. Güç, J.W. Pollard, Redefining macrophage and neutrophil biology in the metastatic cascade, Immunity 54 (5) (2021) 885–902.
[8] M. Orecchioni, Y. Ghosheh, A.B. Pramod, K. Ley, Macrophage polarization: different gene signatures in M1(LPS+) vs. Classically and M2(LPS-) vs. Alternatively activated macrophages, Front. Immunol. 10 (2019) 1084.
[9] B. Kirk, J. Feehan, G. Lombardi, G. Duque, Muscle, bone, and fat crosstalk: the biological role of myokines, osteokines, and adipokines, Curr. Osteoporos. Rep. 18 (4) (2020) 388–400.
[10] G. Hu, Y. Su, B.H. Kang, Z. Fan, T. Dong, D.R. Brown, J. Cheah, K.D. Wittrup, J. Chen, High-throughput phenotypic screen and transcriptional analysis identify new compounds and targets for macrophage reprogramming, Nat. Commun. 12 (1) (2021) 773.
[11] T.A. Wynn, K.M. Vannella, Macrophages in tissue repair, regeneration, and fibrosis, Immunity 44 (3) (2016) 450–462.
[12] C. Varol, A. Mildner, S. Jung, Macrophages: development and tissue specialization, Annu. Rev. Immunol. 33 (2015) 643–675.
[13] C.E. Witherel, K. Sao, B.K. Brisson, B. Han, S.W. Volk, R.J. Petrie, L. Han, K.L. Spiller, Regulation of extracellular matrix assembly and structure by hybrid M1/M2 macrophages, Biomaterials 269 (2021), 120667.
[14] X. Hu, S. Mei, F. Wang, S. Tang, D. Xie, C. Ding, W. Du, J. Zhao, L. Yang, Z. Wu, J. Wei, A microporous surface containing Si(3)N(4)/Ta microparticles of PEKK exhibits both antibacterial and osteogenic activity for inducing cellular response and improving osseointegration, Bioact. Mater. 6 (10) (2021) 3136–3149.
[15] B.R. Levine, S. Sporer, R.A. Poggie, C.J. Della Valle, J.J. Jacobs, Experimental and clinical performance of porous tantalum in orthopedic surgery, Biomaterials 27 (27) (2006) 4671–4681.
[16] Y. Liu, C. Bao, D. Wismeijer, G. Wu, The physicochemical/biological properties of porous tantalum and the potential surface modification techniques to improve its clinical application in dental implantology, Mater. Sci. Eng. C Mater. Biol. Appl. 49 (2015) 323–329.
[17] C. Luo, C. Wang, X. Wu, X. Xie, C. Wang, C. Zhao, C. Zou, F. Lv, W. Huang, J. Liao, Influence of porous tantalum scaffold pore size on osteogenesis and osteointegration: a comprehensive study based on 3D-printing technology, Mater. Sci. Eng. C Mater. Biol. Appl. 129 (2021), 112382.
[18] T. Lei, H. Qian, P. Lei, Y. Hu, The increased oxygen content in tantalum leads to decreased bioactivity and osteogenic ability of tantalum implants, Biomater. Sci. 9 (4) (2021) 1409–1420.
[19] P. Lei, H. Qian, T. Zhang, T. Lei, Y. Hu, C. Chen, K. Zhou, Porous tantalum structure integrated on Ti6Al4V base by Laser Powder Bed Fusion for enhanced bony-ingrowth implants: *in vitro* and *in vivo* validation, Bioact. Mater. 7 (2022) 3–13.
[20] H. Zhu, X. Ji, H. Guan, L. Zhao, L. Zhao, C. Liu, C. Cai, W. Li, T. Tao, J.E. Reseland, H.J. Haugen, J. Xiao, Tantalum nanoparticles reinforced polyetheretherketone shows enhanced bone formation, Mater. Sci. Eng. C Mater. Biol. Appl. 101 (2019) 232–242.
[21] Z. Zhao, M. Wang, F. Shao, G. Liu, J. Li, X. Wei, X. Zhang, J. Yang, F. Cao, Q. Wang, H. Wang, D. Zhao, Porous tantalum-composited gelatin nanoparticles hydrogel integrated with mesenchymal stem cell-derived endothelial cells to construct vascularized tissue *in vivo*, Regen. Biomater 8 (6) (2021), rbab051.
[22] X. Hu, S. Mei, F. Wang, J. Qian, D. Xie, J. Zhao, L. Yang, Z. Wu, J. Wei, Implantable PEKK/tantalum microparticles composite with improved surface performances for regulating cell behaviors, promoting bone formation and osseointegration, Bioact. Mater. 6 (4) (2021) 928–940.
[23] X. Lin, S. Wang, M. Sun, C. Zhang, C. Wei, C. Yang, R. Dou, Q. Liu, B. Xiong, miR-195-5p/NOTCH2-mediated EMT modulates IL-4 secretion in colorectal cancer to affect M2-like TAM polarization, J. Hematol. Oncol. 12 (1) (2019) 20.
[24] J. Voss, C.A. Ford, S. Petrova, L. Melville, M. Paterson, J.D. Pound, P. Holland, B. Giotti, T.C. Freeman, C.D. Gregory, Modulation of macrophage antitumor potential by apoptotic lymphoma cells, Cell Death Differ. 24 (6) (2017) 971–983.
[25] L. Ellis, V. Gilston, C.C. Soo, C.J. Morris, B.L. Kidd, P.G. Winyard, Activation of the transcription factor NF-kappaB in the rat air pouch model of inflammation, Ann. Rheum. Dis. 59 (4) (2000) 303–307.
[26] A. Shapouri-Moghaddam, S. Mohammadian, H. Vazini, M. Taghadosi, S.A. Esmaeili, F. Mardani, B. Seifi, A. Mohammadi, J.T. Afshari, A. Sahebkar, Macrophage plasticity, polarization, and function in health and disease, J. Cell. Physiol. 233 (9) (2018) 6425–6440.
[27] Y. Sun, J. Li, X. Xie, F. Gu, Z. Sui, K. Zhang, T. Yu, Macrophage-osteoclast associations: origin, polarization, and subgroups, Front. Immunol. 12 (2021), 778078.
[28] Y. Yao, X. Cai, F. Ren, Y. Ye, F. Wang, C. Zheng, Y. Qian, M. Zhang, The macrophage-osteoclast Axis in osteoimmunity and osteo-related diseases, Front. Immunol. 12 (2021), 664871.
[29] Y.H. Lin, Y.H. Wang, Y.J. Peng, F.C. Liu, G.J. Lin, S.H. Huang, H.K. Sytwu, C.P. Cheng, Interleukin 26 skews macrophage polarization towards M1 phenotype by activating cJUN and the NF-κB pathway, Cells 9 (4) (2020).
[30] C. Ni, J. Zhou, N. Kong, T. Bian, Y. Zhang, X. Huang, Y. Xiao, W. Yang, F. Yan, Gold nanoparticles modulate the crosstalk between macrophages and periodontal ligament cells for periodontitis treatment, Biomaterials 206 (2019) 115–132.
[31] E. Yeini, P. Ofek, S. Pozzi, N. Albeck, D. Ben-Shushan, G. Tiram, S. Golan, R. Kleiner, R. Sheinin, S. Israeli Dangoor, S. Reich-Zeliger, R. Grossman, Z. Ram, H. Brem, T.M. Hyde, P. Magod, D. Friedmann-Morvinski, A. Madi, R. Satchi-Fainaro, P-selectin axis plays a key role in microglia immunophenotype and glioblastoma progression, Nat. Commun. 12 (1) (2021) 1912.
[32] G.R. Pidwill, J.F. Gibson, J. Cole, S.A. Renshaw, S.J. Foster, The role of macrophages in Staphylococcus aureus infection, Front. Immunol. 11 (2020), 620339.
[33] W. Liu, M. Ma, Z. Lei, Z. Xiong, T. Tao, P. Lei, Y. Hu, X. Jiang, J. Xiao, Intra-articular injectable hydroxypropyl chitin/hyaluronic acid hydrogel as bio-lubricant to attenuate osteoarthritis progression, Mater. Des. 217 (2022), 110579.
[34] J.R. Nakkala, Z. Li, W. Ahmad, K. Wang, C. Gao, Immunomodulatory biomaterials and their application in therapies for chronic inflammation-related diseases, Acta Biomater. 123 (2021) 1–30.
[35] Z. Xu, B. Liang, J. Tian, J. Wu, Anti-inflammation biomaterial platforms for chronic wound healing, Biomater. Sci. 9 (12) (2021) 4388–4409.
[36] S. Han, H. Gao, S. Chen, Q. Wang, X. Li, L.J. Du, J. Li, Y.Y. Luo, J.X. Li, L.C. Zhao, J. Feng, S. Yang, Procyanidin A1 alleviates inflammatory response induced by LPS through NF-κB, MAPK, and Nrf2/HO-1 pathways in RAW264.7 cells, Sci. Rep. 9 (1) (2019), 15087.
[37] J. Li, Y. Li, B. Gao, C. Qin, Y. He, F. Xu, H. Yang, M. Lin, Engineering mechanical microenvironment of macrophage and its biomedical applications, Nanomedicine (Lond) 13 (5) (2018) 555–576.
[38] J. Jiang, W. Liu, Z. Xiong, Y. Hu, J. Xiao, Effects of biomimetic hydroxyapatite coatings on osteoimmunomodulation, Mater Sci Eng C Mater Biol Appl (2022), 112640.
[39] K. Hamidzadeh, S.M. Christensen, E. Dalby, P. Chandrasekaran, D.M. Mosser, Macrophages and the recovery from acute and chronic inflammation, Annu. Rev. Physiol. 79 (2017) 567–592.
[40] S.C. Funes, M. Rios, J. Escobar-Vera, A.M. Kalergis, Implications of macrophage polarization in autoimmunity, Immunology 154 (2) (2018) 186–195.
[41] A. Mantovani, S. Sozzani, M. Locati, P. Allavena, A. Sica, Macrophage polarization: tumor-associated macrophages as a paradigm for polarized M2 mononuclear phagocytes, Trends Immunol. 23 (11) (2002) 549–555.
[42] X. Sun, K. Li, R. Zha, S. Liu, Y. Fan, D. Wu, M. Hase, U.K. Aryal, C.C. Lin, B.Y. Li, H. Yokota, Preventing tumor progression to the bone by induced tumor-suppressing MSCs, Theranostics 11 (11) (2021) 5143–5159.
[43] A.P. West, I.E. Brodsky, C. Rahner, D.K. Woo, H. Erdjument-Bromage, P. Tempst, M.C. Walsh, Y. Choi, G.S. Shadel, S. Ghosh, TLR signalling augments macrophage bactericidal activity through mitochondrial ROS, Nature 472 (7344) (2011) 476–480.
[44] F. Zhou, J. Mei, X. Han, H. Li, S. Yang, M. Wang, L. Chu, H. Qiao, T. Tang, Kinsenoside attenuates osteoarthritis by repolarizing macrophages through inactivating NF-κB/MAPK signaling and protecting chondrocytes, Acta Pharm. Sin. B 9 (5) (2019) 973–985.
[45] J. Hu, H. Wang, X. Li, Y. Liu, Y. Mi, H. Kong, D. Xi, W. Yan, X. Luo, Q. Ning, X. Wang, Fibrinogen-like protein 2 aggravates nonalcoholic steatohepatitis via interaction with TLR4, eliciting inflammation in macrophages and inducing hepatic lipid metabolism disorder, Theranostics 10 (21) (2020) 9702–9720.
[46] R. Zhou, A.S. Yazdi, P. Menu, J. Tschopp, A role for mitochondria in NLRP3 inflammasome activation, Nature 469 (7329) (2011) 221–225.
[47] Y. Yang, L. Guo, Z. Wang, P. Liu, X. Liu, J. Ding, W. Zhou, Targeted silver nanoparticles for rheumatoid arthritis therapy via macrophage apoptosis and Re-polarization, Biomaterials 264 (2021), 120390.